Springer

Journal of Mechanical Science and Technology 23 (2009) 1536~1543

Journal of Mechanical Science and Technology

www.springerlink.com/content/1738-494x
DOI 10.1007/s12206-009-0113-1

Design and analysis of a twisting-type thermal actuator for micromirrors †

Dong Hyun Kim[1], Kyung Su Oh[1] and Seungho Park[2,*]

[1]*Department of Mechanical Engineering, Hongik University, Seoul, Korea*
[2]*Department of Mechanical and System Design Engineering, Hongik University, Seoul, Korea*

(Manuscript Received December 31, 2007; Revised January 5, 2009; Accepted January 21, 2009)

Abstract

This paper reports the design of a novel twisting-type micromirror actuation system. The actuating mechanism for driving the micromirror combines two paralleled bimorph actuators bending in opposite directions for rotational control of the micromirror. Each actuator is structured by gold and silicon dioxide or nickel and silicon nitride thin films with embedded polysilicon line heaters. With a size of only 15μm in width, 1.3μm in thickness, and 100μm in length, two bimorph actuators can result in a vertical displacement of 25μm at 10 volts dc with the span of 120μm, and thus the micromirror can rotate by angles over 20°, which is a significant improvement, compared to conventional tilting-type micromirrors.

Keywords: Micromirror; MEMS; Bimorph thermal actuator; Twisting-mode

1. Introduction

Micromirrors have been demonstrated for a wide variety of applications, such as optical display, optical modulator, scanner, bio-chips, biomedical imaging, laser beam steering, etc. [1]. Further promising applications for micromirrors can be found in the field of optical switches. Advantages of using micromirrors over conventional optical switches include their small size, high speed, low power consumption, and the potential for low cost through batch fabrication [2, 3].

Currently, numerous types of micro actuators are commercially available and most of them are categorized by driving mechanisms in four ways: electrostatic, electromagnetic, piezoelectric and thermal expansion. In general, the tilting angles of micromirrors controlled by electrostatic or electromagnetic actuation are small, and to achieve large angles, it is necessary to either apply a large voltage of over several tens or to operate the devices in a resonant mode [4-9]. On the other hand, piezoelectric and thermal expansion actuators are known to produce large forces and large displacements [10, 11]. Piezoelectric materials, however, are not routinely supported in the fabrication processes offered by commercial MEMS foundries. Thermal actuators for micro system applications have been demonstrated as driving units of micromirrors and they typically use Joule heating as the power source, which generally works at lower voltages than other micro actuation mechanisms.

This study deals with bimorph actuators, whose mechanism is achieved by the difference of the thermal expansion between two adjacent materials. Bimorph actuators based on the bimetal effect are preferred due to their large actuation range at low voltages and simplicity in fabrication.

While micromirrors run by bimorph actuators, as shown in the available literature [12-15], are able to work fast at few kHz with low operation voltages, their tilting angles are relatively small (about 10 de-

† This paper was recommended for publication in revised form by Associate Editor Dongsik Kim

*Corresponding author. Tel.: +82 2 320 1632, Fax.: +82 2 322 7003
E-mail address: spark@hongik.ac.kr

grees). A recent design [16] demonstrates large tilting angles using serial connection between actuators and mirror but only in resonance modes. Although operation voltages could be lowered, their performance for large actuation of current available micromirrors remains to be improved. For that reason, we have investigated thermal actuators for large tilting angles and devised a novel twisting-type actuation mechanism. Here, we have analyzed bimorph actuators for rotational control of the micromirror to optimize the design for a large deflection and thus a large controllable angle of a micromirror at low voltages.

2. Micromirror system

2.1 Design of micromirror systems

Fig. 1 schematically illustrates the micromirror system with a newly designed mechanism. The system consists of two micro actuators of 15μm in width b and 100μm in length L_b, a connection beam between the end-tips of two actuators and the micromirror plate is hanging at the center of the connection beam. Each actuator consists of metal and silicon composite thin-films with poly-silicon line heaters embedded. Two actuators have the same shape and size, but their structures are symmetric across the micromirror plane, and thus they can bend oppositely from each other when they are heated. Therefore, the actuation range of the current system is increased twice as much as that for a conventional system.

Since the mirror is placed at the center of the connection beam, it will rotate without any translational movements.

2.2 Materials for micromirror systems

While common materials for mirrors are aluminum, silver or mercury, they are not acceptable for micromirrors because aluminum and silver are readily oxidized and mercury is difficult to coat. Furthermore, aluminum and silver have low melting temperatures, which imposes serious problems on the thermal actuation mechanism. Therefore, materials for micromirrors must satisfy quite tight design criteria, such as stability at high temperatures, high yielding stress, suitability for microfabrication, material compatibility, etc. In this respect, gold and nickel are widely applied for micromirrors, since they are both stable at high temperatures and melt at temperatures over thousands of degree Celsius.

The bimorphic structure for thermal actuation of micromirrors demands two different materials of quite different thermal expansion properties. Here, the material of high expansion rates such as metals can be used for micromirrors as well as one component of actuators. The material for another part of the bimorphic structure must have similar mechanical properties except for thermal expansion rates. Silicon dioxide is usually applied as the partner material of gold and silicon nitride is as that of nickel. In this paper, therefore, Au/SiO_2 and Ni/SiN_x actuators are analyzed and Table 1 shows the important properties of those materials.

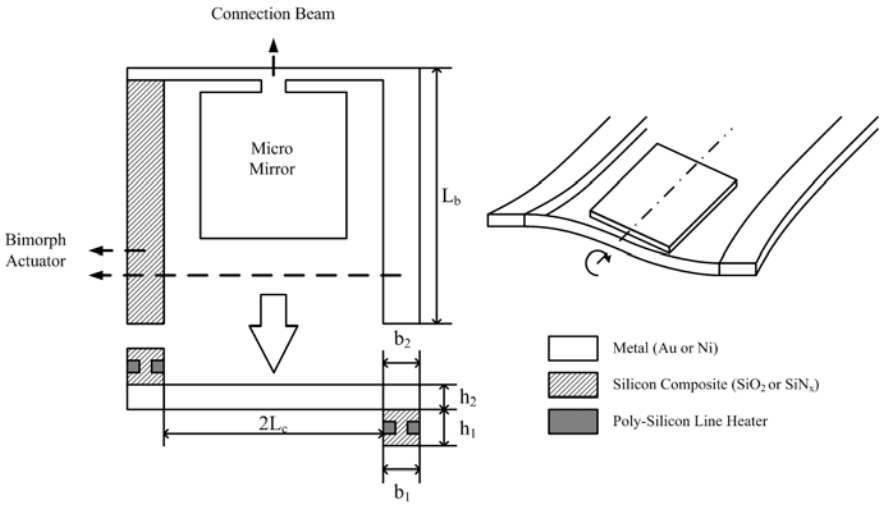

Fig. 1. Micromirror system with two bimorph actuators: top and cross-sectional views and rotational-controlling stage of the micromirror.

2.3 Analysis for actuation system

A large bimorph actuation requires big differences in thermal expansion coefficients between the two-layered materials. Here, those for Au and Ni are much larger than those of SiO_2 and SiN_x, as compared in Table 1. Difference in thermal expansion rate imposes shear stress at the interface of two layers. Since the distributed shear stress has the same effect on the layer as a concentrated force does on the end of the beam, the curvature of bimorph actuators can be derived by the elastic theory. Eq. (1) derived by Chu et al. [17] predicts the curvature of a bimorph actuator when the material is isotropic and the bond between two layers is sufficiently strong. Theoretically, Eq. (1) is reliable, only when the layer thickness is much smaller than the radius of curvature.

$$\frac{1}{\rho} = \eta \Delta T \tag{1}$$

$$\eta = \frac{6E_1E_2b_1b_2h_1h_2(h_1+h_2)(\alpha_2-\alpha_1)}{(E_1b_2h_1^2)^2+(E_2b_2h_2^2)^2+2E_1E_2b_1b_2h_1h_2(2h_1^2+3h_1h_2+2h_2^2)} \tag{2}$$

where subscripts 1 and 2 designate the lower and upper layers, and ΔT denotes the deviation from the reference temperature.

Fig. 2 compares the radii of actuator curvature with respect to the thickness ratio of the layers for unit temperature increase and implies that both Au/SiO_2 and Ni/SiN_x actuators have the smallest radii of curvature around 0.6. Here, 0.6 is used for the thickness ratio, h_2/h_1. The total thickness of each bimorph actuator beam is assumed as 1.3μm (0.5μm for metal and 0.8μm for silicon composite), which limits the natural deformation of the bimorph actuator beam by the total weight of the micromirror system less than 1% of its length.

To estimate the bimorph-beam deflections, δ, Eq. (3) must be applied with Eq. (1),

$$\frac{d^2\delta(x)}{dx^2} = \frac{1}{\rho} \tag{3}$$

Here, boundary conditions for Eq. (3) are given as,

$$\delta(0) = 0 \tag{4}$$

Table 1. Properties of materials used for the design micromirror systems.

	Au [20]	Ni [21]	SiO_2 [17, 18]	SiN_x [17, 18]
Elastic Modulus [GPa]	55	180	70	323
Poisson Ratio	0.42	0.31	0.17	0.23
Coefficient of Thermal Expansion [$10^{-7}K^{-1}$]	142	133	3.5	30
Thermal Conductivity [W/mK]	315	164	0.15	15

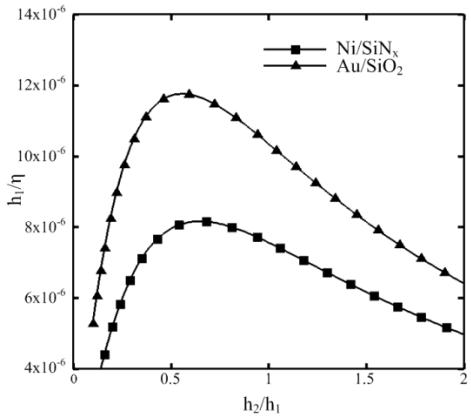

Fig. 2. Radius of curvature for bimorph beams with respect to thickness ratios of two layers.

$$\left.\frac{d\delta}{dx}\right|_{x=0} = 0 \tag{5}$$

To predict the deflection of the bimorph beam, it is necessary to know temperature distributions along the beam. To simplify the analysis, the actuator can be assumed as a fin and one-dimension thermal analysis can be applied, as given in Eq. (6)

$$\frac{d^2T}{dx^2} - \frac{HP}{A\kappa_b}T = -\frac{q_J}{k_b} - \frac{HPT_a}{A\kappa_b} \tag{6}$$

where the volumetric heat generation in the beam is $q_J = V^2/RL_b^2$. The boundary conditions for Eq. (6) are given as

$$-\kappa_b A\left.\frac{dT}{dx}\right|_{x=0} = \frac{(T_a - T(0))}{R_T} \tag{7}$$

$$-\kappa_b A\left.\frac{dT}{dx}\right|_{x=L_b} = H_{fin}A(T(L_b) - T_a) \tag{8}$$

Here, R_T is the effective thermal resistance between the anchor and surroundings (substrate), modeled as

$$R_T = \frac{d_T}{\kappa_{sub} A} \tag{9}$$

where d_T is the gap distance between bimorph actuator and the substrate.

For macro-scale systems the convection heat transfer coefficient in Eq. (6) is usually less than 100 W/m^{2}K for calm air. However, in a micro-scale system, pure natural convection is quite suppressed and instead the conduction through the air gap between the microstructures becomes dominant and the corresponding heat transfer coefficient reaches over 10,000 W/m^{2}K, which is extremely larger than those for macro-scale systems [18-29]. By solving Eq. (6), temperature distribution along to the beam is given as,

$$T(x) = C_1 e^{\gamma x} + C_2 e^{-\gamma x} + \frac{q_J A}{HP} + T_a \tag{10}$$

where

$$\gamma = \sqrt{\frac{HP}{A\kappa_b}} \tag{11}$$

$$C_1 = \frac{\frac{q_J A}{HP}\left[\left(R_T\gamma+1\right)H_{fin}A - \left(\gamma + H_{fin}A\right)e^{-\gamma L_b}\right]}{\left[\left(R_T\gamma+1\right)\left(\gamma - H_{fin}A\right)e^{\gamma L_b} - \left(R_T\gamma-1\right)\left(\gamma + H_{fin}A\right)e^{-\gamma L_b}\right]} \tag{12}$$

$$C_2 = \frac{\frac{q_J A}{HP}\left[\left(R_T\gamma-1\right)H_{fin}A - \left(\gamma - H_{fin}A\right)e^{\gamma L_b}\right]}{\left[\left(R_T\gamma+1\right)\left(\gamma - H_{fin}A\right)e^{\gamma L_b} - \left(R_T\gamma-1\right)\left(\gamma + H_{fin}A\right)e^{-\gamma L_b}\right]} \tag{13}$$

Using Eqs. (1), (3), and (10), the deflection of the bimorph beam can be calculated theoretically as follows:

$$\delta(x) = \frac{\eta}{\gamma^2}\left[C_1 e^{\gamma x} + C_2 e^{-\gamma x}\right] + \frac{q_J A}{2HP}x^2 - \frac{\eta}{\gamma}\left[C_1 - C_2\right]x - \frac{\eta}{\gamma^2}\left[C_1 + C_2\right] \tag{14}$$

Schematically Fig. 1 illustrates how the micromirror works. Bimorphic forces can be treated as concentrated forces imposed on the end part of each actuator. These forces make the actuation beams bend up and down, respectively, and thus the connection beam rotates with slight bending. The rotation of the micromirror, therefore, is the outcome of these two effects, as shown in Fig. 3: rotating and bending of the connection beam.. The deflection and rotating angle of the micromirror can be obtained from the load-stiffness matrix for the micromirror system, given by,

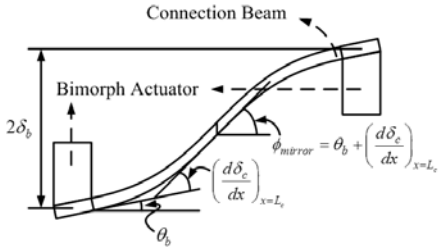

Fig. 3. Deformations of bimorph actuation beams and a connection beam for twisting-type micromirrors systems.

$$\begin{bmatrix} K_b & K_c & 0 & 0 \\ 1 & -1 & -L_c & 0 \\ L_b K_b & 0 & 0 & -K_{T_c} \\ 0 & L_c K_c & -K_{T_b} & 0 \end{bmatrix}\begin{bmatrix} \delta_b \\ \delta_c \\ \theta_b \\ \theta_c \end{bmatrix} = \begin{bmatrix} F_b \\ 0 \\ 0 \\ 0 \end{bmatrix} \tag{15}$$

$$K_b = \frac{3EI_b}{L_b^3}, \quad K_c = \frac{3E_c I_c}{L_c^3}, \quad K_{Tb} = \frac{GJ_b}{L_b}, \quad K_{Tc} = \frac{G_c J_c}{L_c} \tag{16}$$

$$EI_b = \frac{(E_1 b_1 h_1^2)^2 + (E_2 b_2 h_2^2)^2 + 2E_1 E_2 b_1 b_2 h_1 h_2 (2h_1^2 + 3h_1 h_2 + 2h_2^2)}{12(E_1 b_1 h_1 + E_2 b_2 h_2)} \tag{17}$$

$$GJ_b = \frac{1}{12}\left(G_1 h_1 + G_2 h_2\right)b^3 \tag{18}$$

$$F_b = \frac{3EI_b \delta(L_b)}{L_b^3} \tag{19}$$

where F_b is the equivalent concentrated force imposed on each actuator induced by the bimorph effect. By solving Eq. (15), the angles and deflections can be obtained as follows:

$$\delta_b = \frac{3EI_b \delta(L_b)\left(K_{Tb} + L_c^2 K_c\right)}{L_b^3\left(K_b K_{Tb} + K_c K_{Tc} + L_c^2 K_b K_c\right)} \tag{20}$$

$$\delta_c = \frac{3EI_b \delta(L_b) K_{Tb}}{L_b^3\left(K_b K_{Tb} + K_c K_{Tc} + L_c^2 K_b K_c\right)} \tag{21}$$

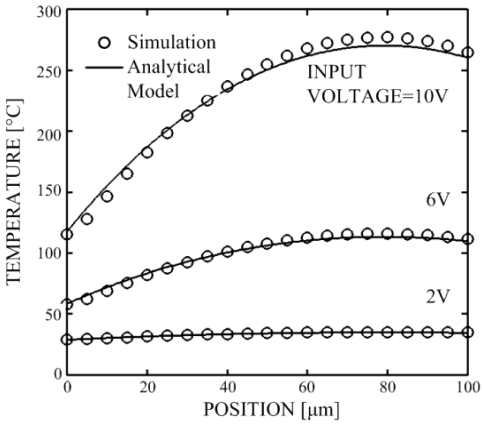

Fig. 4. Analytical results compared to simulation model for temperature distributions of an Au/SiO_2 bimorph beam.

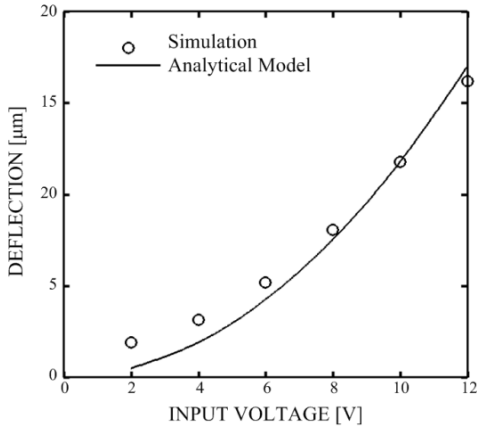

Fig. 5. Analytical results compared to simulation model for deflections of Au/SiO_2 bimorph beams.

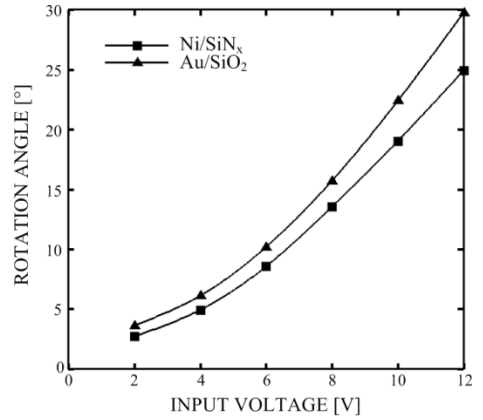

Fig. 6. Maximum rotation angles of micromirrors with respect to input voltages.

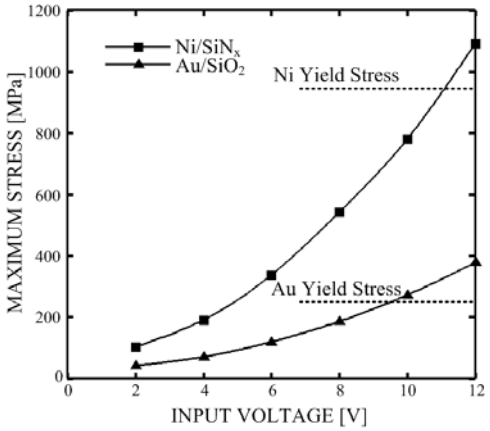

Fig. 7. Stresses of bimorph actuators of a micromirror system with respect to input voltages.

$$\theta_b = \frac{3EI_b\delta(L_b)L_cK_c}{L_b^3\left(K_bK_{Tb}+K_cK_{Tc}+L_c^2K_bK_c\right)} \tag{22}$$

$$\theta_c = \frac{3EI_b\delta(L_b)\left[L_bK_b\left(K_{Tb}+L_c^2K_c\right)\right]}{L_b^3K_{Tc}\left(K_bK_{Tb}+K_cK_{Tc}+L_c^2K_bK_c\right)} \tag{23}$$

$$\phi_{mirror} = \theta_b + \left.\frac{d\delta_c}{dx}\right|_{x=L_C} = \frac{6EI_b\delta(L_b)L_c^2K_c + 9EI_b\delta(L_b)K_{Tb}}{2L_cL_b^3\left(K_bK_{Tb}+K_cK_{Tc}+L_c^2K_bK_c\right)} \tag{24}$$

Here, δ_b and δ_c indicate the deflections and θ_b and θ_c indicate the twisting angles of the bimorph actuator and the connection beam, respectively. Fig. 3 illustrates the rotation angle of the micro mirror, expressed in Eq. (24). From Eq. (24), we can estimate the length of the connection beam to maximize the rotation angle, which results in $2L_c$ 120μm for this simulation.

3. Simulation

In this paper, a commercial simulation package for MEMS systems, Intellisuite [20], has been used and the simulation results are compared to the results from the analytic models given in Sec. 2. The simulation uses the ideal structure of the bimorph beam with line heaters embedded, as shown in Fig. 1, while the analytical model omits the line heaters and assumes uniform heating in layer 1.

Fig. 4 compares the temperature distributions along

the Au/SiO_2 actuator beams obtained from the simulation and the analytic model and implies that their results are quite close to each other in spite of slightly different structures. The temperature rises are quite small for input voltages less than 2 volts and are sufficiently large for that greater than 6 volts.

Fig. 5 compares the deflections of Au/SiO_2 bimorph beam with respect to input voltages. While the deflections from the simulation and the analytic model are quite different for small input voltages where actuation is very small, they are close to each other for large voltages, which is practically important. This slight deviation is due to discrepancy of the structures of two models. While the analytical model is a pure bimorph structure that has only Au and SiO_2 or Ni and SiN_x layers, the simulation model uses the embedded poly-Si line heaters. Since poly-Si is stiffer and expands more than SiO_2, the embedded poly-Si structure results in smaller bimorphic sensitivities.

Temperature and stress in a thermal bimorph beam usually limit the operational range of the actuators. Here, maximum operation temperatures of both Au/SiO_2 and Ni/SiN_x actuators at input voltages around 10 volts are much lower than their melting temperatures, as shown in Fig. 4. Yield stresses of gold and nickel are about 250 MPa and 950 MPa [21-22], respectively, while those of SiO_2 and SiN_x are over 1 GPa. Hence, the major design constraint parameter of the bimorph actuator is the yield stress of the metal layer. Fig. 6 shows maximum stresses with respect to the input voltages for Au/SiO_2 and Ni/SiN_x actuators, and Fig. 7 indicates the region of maximum stress that is the inner corner region of the connection beam. The maximum input voltages to cause yield are about 9.5 volts for an Au/SiO_2 actuator while 11.5 volts for a Ni/SiN_x actuator. Although nickel can bear very high stresses, it has much higher elastic modulus than gold does. Therefore, operational voltages are limited by about 10 volts for both actuators. Fig. 7 shows the simulation result of the Au/SiO_2 actuation system and the stress distribution. As the stresses are confined in the corner region of the connection and bimorph beams, design modification around the corner region is needed to decrease the stress and to increase the operational range.

The deflection δ_b and rotating angles ϕ_{mirror} of Au/SiO_2 and Ni/SiN_x actuator systems, depicted in Fig. 3, are compared in Figs. 8 and 9, respectively. Fig. 8 implies that combined effects from elastic modulus, thermal expansion coefficient, and electric

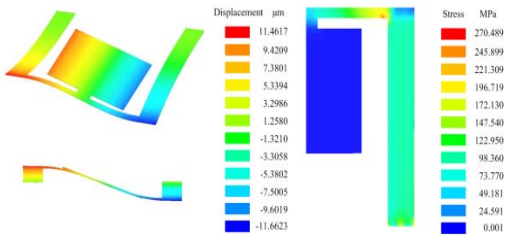

(a) (b)

Fig. 8. Simulation results of an Au/SiO_2 micromirror system: (a) operation stage of the micromirror and (b) stress distribution under input voltage of 10 volts.

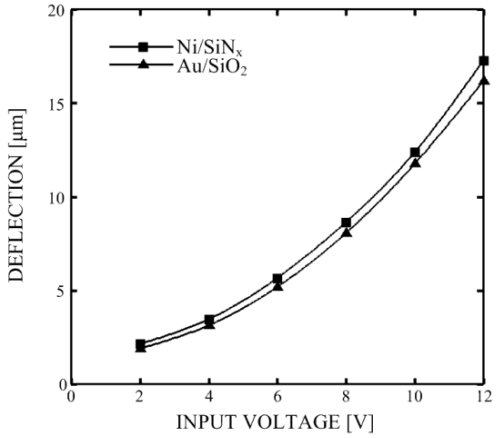

Fig. 9. Maximum deflections of bimorph actuators of a micromirror system with respect to input voltages.

and thermal resistance result in similar deflections of the two different actuation systems (see Eq. (1)). Fig. 9, however, shows that the rotating angles for the Au/SiO_2 actuator system are slightly greater than those for the Ni/SiN_x system and indicates that the maximum operational angles can reach up to 20° for Au/SiO_2 actuators and 18° for Ni/SiN_x actuators without yield. This is due to the fact that the bimorph actuator is not only bent but also twisted, as pointed out in Eq. (24) and shown in Fig. 7(a). Since one of important factors governing the twisting angle, θ_b, is the stiffness ratio of connection and bimorph actuator beams and this ratio for the Au/SiO_2 system is 0.017 while the Ni/SiN_x system is 0.05, the Au/SiO_2 micromirror rotates greater than the Ni/SiN_x micromirror does.

4. Conclusions

A twisting-type bimorph actuation system is designed and analyzed for efficient actuation of mi-

cromirrors. Two bimorphic actuators structured by metal and silicon composite thin films can bend oppositely from each other upon heating, and the micromirror attached at the center region of the beam connecting the actuators can rotate accordingly. The bimorphic materials for the actuator beam are Au/SiO_2 or Ni/SiN_x pairs, which satisfy some particular design and fabrication criteria for micromirror systems.

A simple analytic model based on the one-dimensional heat transfer theory for fins and the elastic theory is compared to the simulation results by using Intellisuite, a commercial simulation package for MEMS. Although the models of bimorphic structures are slightly different, the results from the analytic model and simulation are very close to each other.

A simple optimization procedure can suggest that the size of each bimorph actuation beam is 15μm in width, 1.3μm in thickness (0.5μm for metal and 0.8μm for silicon composite), 100μm in length and the length of the connection beam is 120μm, which can admit a micromirror smaller than 100μm in width and in length.

Since the temperatures of the bimorph beams are much smaller than their melting temperatures for input voltages under normal operations, the thermal design criterion is not critical. Instead, the maximum stresses greater than the yield points can limit the actuation ranges and suggest that maximum input voltages are 9 volts for Au/SiO_2 actuators and 11.5 volts for Ni/SiN_x actuators.

The maximum operational angles can reach up to 20° for Au/SiO_2 actuators and 18° for Ni/SiN_x actuators without yield. The rotating angles for the Au/SiO_2 actuator system are slightly greater than those for the Ni/SiN_x system, while the deflections are very close to each other.

The simulation indicates that stresses are highly confined to the region of inner corner between the actuation and connection beams, which demands further investigation for the relief of stress concentration. In addition, the dynamic characteristics of the current actuation system remain to be explored in future study.

Acknowledgment

This work was supported by the Korea Research Foundation Grant funded by the Korean Government (KRF-2008-313-D00097).

Reference

[1] H. Hujita, Microactuators and Micromachines, *Proceedings of the IEEE*, 86 (8) (1998) 1721-1732.

[2] G. I. Papadimitriou, C. Papazoglou and A. S. Pomportsis, Optical Switching: Switch Fabrics, Techniques, and Architectures, *Journal of Lightwave Technology*, 21 (2) (2003) 384-405.

[3] S. Sundaram, M. Knapczyk, and H. Temkin, All-Optical Switch Based on Digital Micromirrors, *Photonic Technology Letters*, 15 (6) (2003) 807-809.

[4] C. Tsou, W. T. Lin, C. C. Fan and B. C. S. Chou, A Novel Self-Aligned Vertical Electrostatic Combdrives Actuator for Scanning Micromirrors, *Journal of Micromechanics and Microengineering*, 15 (4) (2005) 855-860.

[5] H. Schenk, P. Dürr, D. Kunze, H. Lakner and H. Kück, A Resonantly Excited 2D-Micro-Scanning-Mirror with Large Deflection, *Sensors and Actuators A: Physical*, 89 (1-2) (2001) 104-111.

[6] U. Krishnamoorthy, K. Li, K. Yu, D. Lee, J. P. Heritage and O. Solgaard, Dual-Mode Micromirrors for Optical Phased Array Applications, *Sensors and Aactuators. A, Physical*, 97-98 (2002) 21-26.

[7] A. Nakai, K. Hoshino, K. Matsumoto and I. Shimoyama, Double-Sided Scanning Micromirror Array for Autostereoscopic Display, *Sensors and Actuators A: Physical*, 135 (1) (2007) 80-85.

[8] J. W. Judy and R. S. Muller, Magnetic Microactuation of Torsional Polysilicon Structures, *Sensors and Actuators A: Physical*, 53 (1-3) (1996) 392-397.

[9] A. D. Yalcinkaya, O. Ergeneman and H. Urey, Polymer Magnetic Scanners for Bar Code Applications, *Sensors and Actuators A: Physical*, 135 (1) (2007) 236-243.

[10] H. Kueppers, T. Leuerer, U. Schnakenberg, W. Mokwa, M. Hoffmann, T. Schneller, U. Boettger and R. Waser, PZT thin Films for Piezoelectric Microactuator Applications, *Sensors and Actuators A: Physical*, 97-98 (2002) 680-684.

[11] F. Filhol, E. Defaÿ, C. Divoux, C. Zinck and M. T. Delaye, Resonant Micro-Mirror Excited by a Thin-Film Piezoelectric Actuator for Fast Optical Beam Scanning, *Sensors and Actuators A: Physical*, 123-124 (2002) 483-489.

[12] S. Schweizer, S. Calmes, M. Laudon and P. Renaud, Thermally Actuated Optical Microscanner

with Large Angle and Low Consumption, *Sensors and Actuators A: Physical*, 76 (1-3) (1999) 470-477.
[13] L.-A. Liew, A. Tuantranont and V. M. Bright, Modeling of Thermal Actuation in a Bulk-Micromachined CMOS Micromirror, *Microelectronics Journal*, 31 (9-10) (2000) 791-801.
[14] J. Funk, J. Buhler, J. G. Korvink and H. Baltes, Modeling of Thermomechanical Actuated Micromirror, *Sensors and Actuators A: Physical*, 47 (1/3) (1995) 632-636.
[15] D. O. Popa, B. H. Kang, J. T. Wen, H. E. Stephanou, G. Skidmore and A. Geisberger, Dynamic Modeling and Input Shaping of Thermal Bimorph MEMS Actuators, *Proceedings of IEEE International Conference on Robotics and Automation,* Taipei, Taiwan, September 14-19 (2003) 1470-1475.
[16] A. Jain, H. Qu, S. Todd and H. Xie, A thermal bimorph micromirror with large bi-directional and vertical actuation, *Sensors and Actuators A: Physical*, 122 (1) (2005) 9-15.
[17] W. H. Chu, M. Mehregany and R. L. Mullen, Analysis of Tip Deflection and Force of a Bimetallic Cantilever Microactuator*, Journal of Micromechanics and Microengineering*, 3 (1) (1993) 4-7.
[18] R. W. Johnstone and M. Parameswran, Modelling Surface-Micromachined Electrothermal Actuators, *Canadian Journal of Electrical and Computer Engineering*, 29 (3) (2004) 193-200.
[19] A. Cabal, D. S. Ross, J. A. Lebens and D. P. Trauernicht, Thermal Actuator with Optimized Heater for Liquid Drop Ejectors, *Sensors and Actuators A: Physical*, 123-124 (2005) 531-539.
[20] Intellisuite 8, Intellisense Software Corp, Boston, Massachusetts, USA (2005)
[21] W. Tang, K. Xu, P. Wang, and X. Li, Residual Stress and Crystal Orientation in Magnetron Sputtering Au Films" *Materials Letters*, 57 (20) (2003) 3101-3106.
[22] R. Schwaiger, B. Moser, M. Dao, N. Chollacoop, and S. Suresh, Some Critical Experiments on the Strain-Rate Sensitivity of Nanocrystalline Nickel, *Acta Materialia*, 51 (2003) 5159~5172.

Dong Hyun Kim received his B.S. and M.S. degrees in Mechanical Engineering from Hongik University, Korea, in 2005 and 2007, respectively. Mr. Kim is currently graduate student in the department of Mechanical Engineering at Hongik University in Seoul, Korea. His research interests include micro and nanoscale heat transfer and silicon crystallization technologies for displays.

Kyung Su Oh received his B.S. and M.S. degrees in Mechanical Engineering from Hongik University, Korea, in 2005 and 2007, respectively. Mr. Oh is currently a research scientist at LG Chem. Ltd. His research interests include nanoscale heat transfer, nanotubes and fuel cells and molecular simulation technology.

Seungho Park received his B.S. and M.S. degrees in Mechanical Engineering from Seoul National University, Korea, in 1981 and 1983, respectively. He then received his Ph.D. degree from U.C. Berkeley, U.S.A. in 1989. Dr. Park is currently a Professor at the department of Mechanical and System Design Engineering at Hongik University in Seoul, Korea. He served as a director of general affairs of KSME. Dr. Park's research interests include micro and nanoscale heat transfer, molecular dynamics simulation and silicon crystallization technologies for displays.